Stability improvement of a HVDC transmission link between weak AC systems by Multi-terminal scheme

A F Nnachi[1], Prof J L Munda[1], IEEE Member,
[1]Department of Electrical Engineering
Tshwane University of Technology
Pretoria South Africa

Prof DV Nicolae[1], IEEE Member , Prof A Mpanda Mabwe[2], IEEE Senior Member
[2]Ecole superieure D'Ingenieurs en Electronique et Electrotechnique Amiens
France

***Abstract*— High Voltage Direct Current (HVDC) schemes are becoming a more attractive solution as they have been used extensively in interconnected weak power AC systems.**

But, the problem of voltage stability for weak AC systems interconnected by a DC link is critical especially during islanding conditions. The approach to improve more on the stability of such system would be to device a means of injecting locally controlled dc power on the dc-link transmission corridor forming a radial multi-terminal HVDC. However, continuous injection of DC power on the dc line of the VSC HVDC link though will increase the power transfer capability of the system but should have a limit otherwise it will lead to instability of the system. In this paper, a detailed VSC HVDC model and a simple analytical technique using the principle of uniform loading to determine penetration limit is presented. The techniques is applied to our case study and validated with a simulation result.

Critical contingencies such as sudden island conditions, three-phase to ground fault are simulated with and without DC power penetration. Results show the stability support on the AC side networks by DC power injection on the dc-link.

***Index Terms*—VSC, HVDC, Distributed generation, Multi-terminal**

I. INTRODUCTION

Research has shown that High Voltage Direct Current (HVDC) power transmission suits better the requirements of long distance, power transmission in relation to classical AC transmission lines because no reactive power is produced/consumed by the transmission cable, reducing the losses in the power transmission system [1].

Interconnecting two weak AC systems through HVDC, voltage source converter (VSC) based technology was considered because it can operate in a much weaker network compared to traditional thyristor based HVDC systems. However, several investigations have shown that VSC-HVDC based on vector current control also has problems in maintaining stable operation if the connected ac system is weak [2-4].

From the advent of VSC HVDC with long DC transmission link in power systems, situations have arisen and will be even more frequent in the future, where several distributed generation will be connected on the DC-link for more stable operation, power transfer capability and support especially during critical contingencies.

The integration of very large scale distributed generation (offshore/onshore wind parks or photovoltaic system) into the existing two terminals VSC HVDC transmission corridor without interfering with its main control is a huge challenge. It could begin with radial connections and ends up with fully multi-terminal meshed DC grid. Classical multi-terminal HVDC [5-8], are based on different kinds of control strategy: those which use a master controller to specify certain control of some parameters and those which employ a coordinated control system where no master controller is required.

However, in this case study, the power injection should be small not to interfere with the main control of the HVDC but should be sufficient to aid the system during critical conditions.

In this paper, VSC HVDC model based on vector control, DC line model based on cascaded π-section and proposed analytical method for DG power injection limit on the DC-link is presented.

II. MODELLING AND CONTROL OF VSC HVDC

The VSC based HVDC transmission system mainly consist of two converter stations connected by a dc cable as shown in fig. 1. The magnitude of ac output voltage of the converter is controlled by pulse width modulation (PWM) without changing the magnitude of the dc voltage.

In this paper, the emphasis is not placed on the control scheme rather a standard vector control [9],[10] of VSC HVDC is utilized for the modelling in Matlab/Simulink. The schematic of a VSC HVDC terminal shown in fig. 2 is used for the modeling of the system in d-q reference frame for proper control.

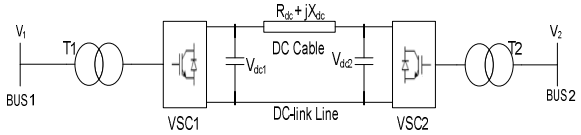

Fig. 1 Schematic representation of VSC based HVDC

978-1-4673-5943-6/13/$31.00 © 2013 IEEE

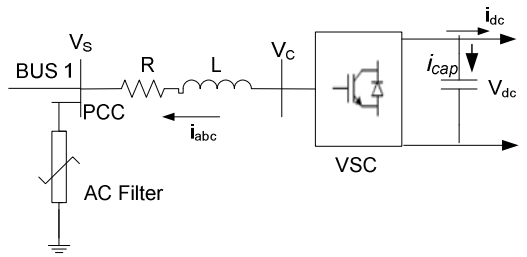

Figure 2 Schematic of a VSC HVDC Terminal

From figure 2, applying Kirchhoff law between the point of common coupling to the source and the converter terminal,

$$V_{Sabc} - V_{cabc} = L\frac{di_{abc}}{dt} + Ri_{abc} \tag{5}$$

L and *r* represent the total inductance and resistance of the transformer and phase reactor.

$$\begin{bmatrix} V_{Sa} \\ V_{Sb} \\ V_{Sc} \end{bmatrix} - \begin{bmatrix} V_{ca} \\ V_{cb} \\ V_{cc} \end{bmatrix} = L\frac{d}{dt}\begin{bmatrix} i_a \\ i_b \\ i_c \end{bmatrix} + R\begin{bmatrix} i_a \\ i_b \\ i_c \end{bmatrix} \tag{6}$$

To simplify the expression of the control mode, AC voltage and AC current in 3-phase static coordinate are transformed to voltage and current in the synchronous *dq0* reference frame through park transformation [11].

Transforming (6) into rotating *dq0* frame based on the transformation

$$[f_{dq0}] = T_{dq0}(\omega t)[f_{abc}] \tag{7}$$

where

$$T_{dq0} = \frac{2}{3}\begin{bmatrix} cos\omega & cos\left(\omega t - \frac{2\pi}{3}\right) & cos\left(\omega t + \frac{2\pi}{3}\right) \\ sin\omega t & sin\left(\omega t - \frac{2\pi}{3}\right) & sin\left(\omega t + \frac{2\pi}{3}\right) \\ \frac{1}{\sqrt{2}} & \frac{1}{\sqrt{2}} & \frac{1}{\sqrt{2}} \end{bmatrix}$$

Where ω is the frequency of the fundamental component in AC network. In order to decouple the active and reactive power controls, the synchronous rotating d-q reference frame will be used for developing the controllers. The d-q transformed equivalent of equation (6) using equation (7) is given by

$$V_{Sdq} - V_{cdq} = L\frac{di_{dq}}{dt} + j\omega Li_{dq} + Ri_{dq} \tag{8}$$

The term $j\omega Li_{dq}$ in (8) represents the time derivative of the synchronous rotation of the *dq* reference frame. It is supposed that system operates symmetrically in steady state condition. So, there are no zero sequence components when 3-phases are balanced.

Rewriting (8)

$$\frac{d}{dt}\begin{bmatrix} i_d \\ i_q \end{bmatrix} = \frac{1}{L}\begin{bmatrix} -R & \omega L \\ -\omega L & -R \end{bmatrix}\begin{bmatrix} i_d \\ i_q \end{bmatrix} + \frac{1}{L}\begin{bmatrix} V_{Sd} \\ V_{Sq} \end{bmatrix} - \frac{1}{L}\begin{bmatrix} V_{cd} \\ V_{cq} \end{bmatrix} \tag{9}$$

The phase locked loop (PLL) provides the angle for *abc-dq/dq-abc* transformation blocks in phase locked with phase voltage at the AC bus. Suppose that the fundamental component of AC bus voltage V_S is in d-axis, therefore V_{Sq} is equal to zero while the magnitude of V_{Sd} is equal to that V_S. This simplifies the equation (9) to (10)

$$\frac{d}{dt}\begin{bmatrix} i_d \\ i_q \end{bmatrix} = \frac{1}{L}\begin{bmatrix} -R & \omega L \\ -\omega L & -R \end{bmatrix}\begin{bmatrix} i_d \\ i_q \end{bmatrix} + \frac{1}{L}\begin{bmatrix} V_{Sd} \\ 0 \end{bmatrix} - \frac{1}{L}\begin{bmatrix} V_{cd} \\ V_{cq} \end{bmatrix} \tag{10}$$

Equation (10) can rewritten as

$$\left.\begin{aligned} V_{cd} - V_{Sd} &= L\frac{di_d}{dt} + Ri_d - \omega Li_q \\ V_{cq} &= L\frac{di_q}{dt} + Ri_q + \omega Li_d \end{aligned}\right\} \tag{11}$$

From (11), the equivalent circuit of the VSC in Synchronized *d-q* reference frame can be shown as in figure 3

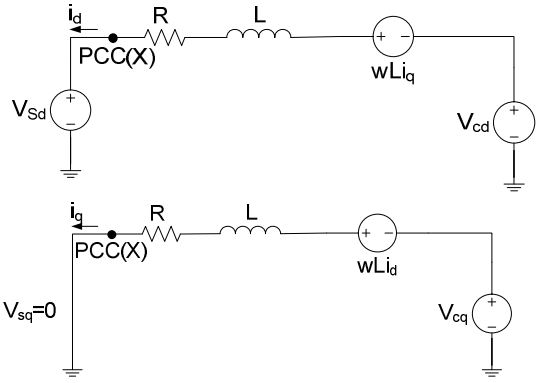

Fig. 3 Equivalent circuit diagram of VSC in synchronous d-q reference frame [10]

Equation (11) shows that the model of the VSC in the synchronous reference frame is a multiple-input multiple output, strongly coupled nonlinear system.

A. Inner Current controller

The inner current controller can be developed based on (10). To decouple the control of i_d and i_q let

$$\left.\begin{aligned} V_{cd} &= -\left(K_p + \frac{1}{T_1 s}\right)(i_{dref} - i_d) + \omega Li_q + V_{Sd} \\ V_{cq} &= -\left(K_p + \frac{1}{T_1 s}\right)(i_{qref} - i_q) - \omega Li_d + V_{Sq} \end{aligned}\right\} \tag{12}$$

Substituting equation (12) into equation (10), the equation becomes

$$\frac{d}{dt}\begin{bmatrix} i_d \\ i_q \end{bmatrix} = \left\{\begin{bmatrix} \frac{1}{L}\begin{bmatrix} -\left[R - \left(k_p + \frac{1}{T_{1s}}\right)\right] & 0 \\ 0 & -\left[R - \left(k_p + \frac{1}{T_{1s}}\right)\right] \end{bmatrix}\begin{bmatrix} i_d \\ i_q \end{bmatrix} + \\ \frac{K_p + \frac{1}{T_{1S}}}{L}\begin{bmatrix} i_{dref} \\ i_{qref} \end{bmatrix} \end{bmatrix}\right\} \tag{13}$$

From (13), the decoupling control is realized. Figure 4 shows the block diagram of VSC-HVDC decoupling controller

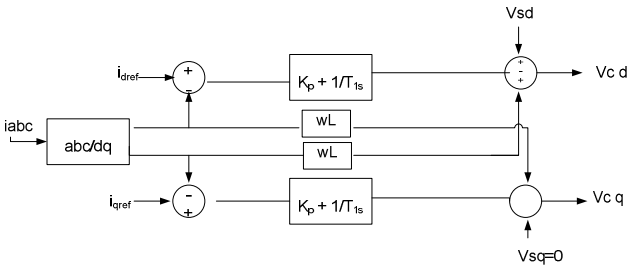

Fig. 4 Control diagram

B. The outer controller

The outer controller constitutes one of DC voltage, active/reactive power and AC voltage control. From the d-q equivalent circuit figure 3, the apparent power injected by the VSC into the network as observed from reference point of connection PCC (X) is given by:

$$S_{dq} = \frac{3}{2} V_{s-dq} i_{dq} = \frac{3}{2}\left(V_{sd} + jV_{sq}\right)\left(i_d - ji_q\right)$$

$$= \frac{3}{2}\left\{\left(V_{sd} i_d + V_{sq} i_q\right) + j\left(V_{sq} i_d - V_{sd} i_q\right)\right\} \quad (14)$$

Since $V_{sq} = 0$, hence active and reactive powers are given by

$$P = \frac{3}{2} V_{sd} i_d \quad (15)$$

$$Q = \frac{-3}{2} V_{sd} i_q \quad (16)$$

For a steady state operation, active power exchange at the AC side (at PCC) will be equal to the power exchange at the DC bus. Mathematically;

$$P_{dq} = P_{DC} \quad (17)$$

A small change in the DC voltage can be approximated as:

$$\Delta V_{DC} = \frac{\Delta q_{cap}}{C} = \frac{1}{C}\int i_{cap}\, dt \quad (18)$$

Where C is the capacitance of the DC bus, q_{cap} is the charge and i_{cap} current going into it. From (17)

$$\frac{3}{2} V_{sd} i_d = V_{DC} i_{cap} + V_{DC} I_{DC} \quad (19)$$

But from (18), $C\frac{d\Delta V_{DC}}{dt} = i_{cap}$

$$\frac{3}{2} V_{sd} i_d = V_{DC} C \frac{d\Delta V_{DC}}{dt} + V_{DC} I_{DC} \quad (20)$$

Therefore

$$\frac{d\Delta V_{DC}}{dt} = \frac{-3V_{sd}}{2CV_{DC}}\left(i_d + \frac{2V_{DC} I_{DC}}{3V_{sd}}\right) \quad (21)$$

Equations (15) and (21) show that active power and DC voltage are correlated by i_d, (16) shows that reactive has direct relation with i_q . The resulting control structures are shown in fig. 5. The active current reference can either be obtained from DC voltage controller or power controller. Therefore a total of four controllers at each converter station or eight controllers for two-terminal VSC based HVDC. Each operating mode requires proper tuning of controller gains in order to achieve satisfactory system performance.

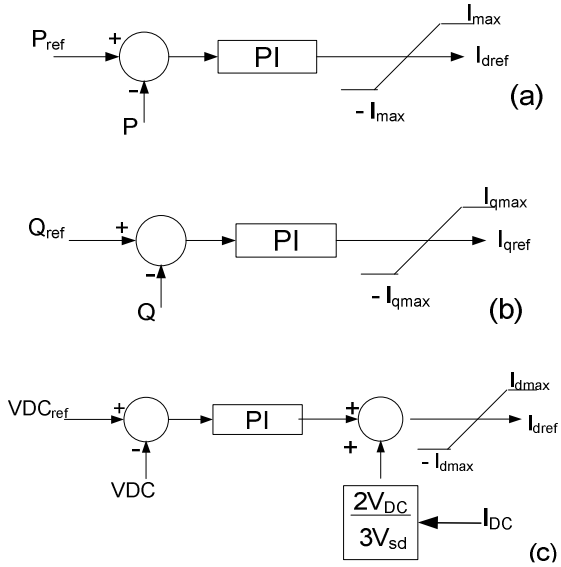

Fig. 5. Outer controllers

The DC current beyond the capacitor bank is feed forward compensated in the DC voltage controller as shown in fig. 5c.

III. DC-LINK TRANSMISSION LINE MODEL

Transmission lines are a vital link in HVDC transmission systems. Its resistance, inductance and capacitance are uniformly distributed along the line. An approximate model of the distributed parameters line obtained by cascading several identical (π) sections as shown in the figure was used in our model.

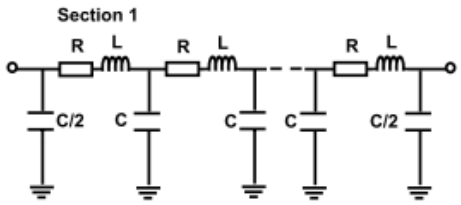

Fig. 6 (π) sections line

The number of sections to be used depends on the frequency range to be represented [13].

IV. DC-LINK POWER INJECTION LIMIT DETERMINATION

DC Power injection on the DC-link of the HVDC system will result to multi-terminal system. Each injection terminal should be locally controlled not to interfere with the main HVDC control. Fig. 7 shows the resultant equivalent circuit of the resulting 3-terminal VSC HVDC for one point of injection.

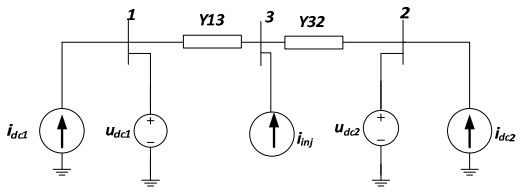

Fig. 7 equivalent circuit of 3terminal VSC HVDC

Fig. 8 shows equivalent circuit of n-terminal radial VSC HVDC obtained as a result of several DG DC power injections along the dc-link of HVDC transmission corridor.

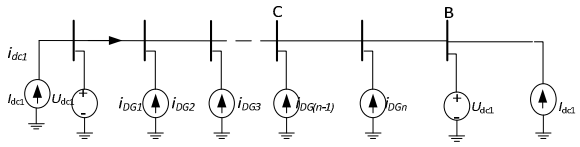

Fig. 8 Equivalent circuit of n-terminal radial VSC HVDC

In order to determine total DG power injection limit, power sensitivity and algebraic technique was proposed in [14].
If the total DG installed capacity is considered to be installed at a particular point on the DC-link, the tolerable power injection limit without affecting the main control of the system is given by

$$P_{DGlimit} = -\frac{U_{DCmax}(U_{DCmax}-U_{DCref})}{rx} + \left(1-\frac{x}{2L}\right)U_{DC2}I_{DC2} \quad (22)$$

Where
$P_{DGlimit}$ = Maximum DG DC power injection for unity reference power of the main control
U_{DCmax} = the upper voltage regulation limit in p.u specified in the control
U_{DCref} = the reference voltage in p.u
r = resistance per unit length of the line
x = distance of from bus 1
L = Total length of the DC-link
U_2 = converter AC output voltage
E_2 = AC bus voltage
X_{th} = the thevenin equivalent reactance of the ac system
U_{dc2} = pu the upper voltage regulation (limit in p.u specified in the inverter control)
$I_{dc2} = I_{rated}$ = pu current reference limit (current set point specified in the inverter control)

V. SIMULATION OF CASE STUDIES

In order to further verify and validate the proposed technique in [14], a typical Caprivi VSC HVDC linking Namibia weak AC network and Zambia weak AC network was modeled and simulated in MATLAB/SIMULINK. The SCR of the two AC networks linked with HVDC was reported in [16] to be about 1.5. Table 1 shows the simulation parameters used for our model. The control settings of the model are as follows:

$U_{dcmax} = 1.05\,p.u;\ U_{dcref} = 0.95; U_{dc2} = 1.05\,pu\ ;\ I_{dc2} = 1pu; r = 0.0139\,pu\ of\ km.$

Table 1Simulation parameter

Data	Parameters
Power rating	300 MW
Overload rating in monopolar mode	350 MW
No of poles	1
AC voltage	Gerus: 400 kV; Zambezi: 330 kV
DC voltage	350 kV
Coupling transformer on both sides (Gerus and Zambezi)	315 MVA
Length of overhead DC line	950 km
Switching frequency of converter valve	1150 kHz
Main reason for choosing HVDC	Long distance weak networks

A. *Dynamic Effect of increase DC power penetration*

The simulations were carried by injecting DC power on the midpoint of the dc-link (x=475 km).
Fig. 9 shows the effect of increasing DG DC power injection on the dc-link. It can be seen that as power injection increases, power transfer from VSC1 remains constant (0.63 pu) until a point of injection limit of 0.57 pu (171 MW), then Pdc1 drops appreciably. Therefore, the limit of DG DC power injection at the middle point of the DC-link is seen by simulation to be 0.57 p.u
From the algebraic equation (35), substituting the control and dc-link parameters, the DG injection limit is calculated thus:

$$P_{DGlimit} = -\frac{1.05(1.05-0.95)}{1.39\times10^{-2}\times475} + \left(1-\frac{475}{2x950}\right)\times1.05\times1$$

$$= 0.787 \text{ p.u}$$

This value is for unity reference power of the control setting, Therefore for reference power of 0.65, $P_{DGmax} = 0.65 \times 0.787 = 0.5\,p.u$ or (150 MW)

Fig. 10 shows the dynamic effect of increase in DC power injection. At 1.17 s, the DC power injection is increased from zero to 118 MW which is below injection limit, hence PDc1 remained constant. However, when the injection increased above the limit at 2 s, it could be seen how the PDC1 decreased substantially and at the same time the voltage increased beyond acceptable limit indicating power and voltage instability respectively.

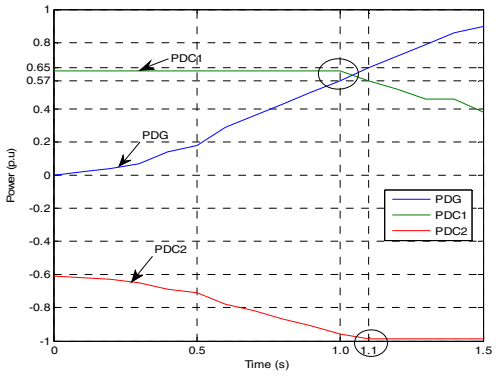

Fig. 9 Effect of increase DG DC power injection

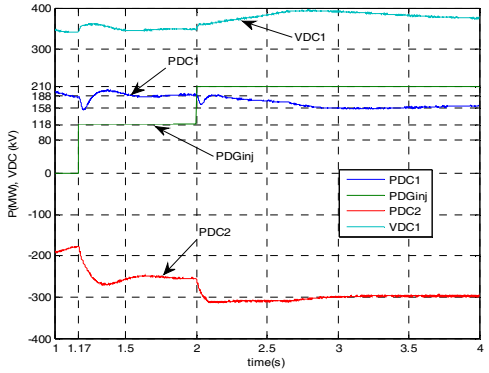

Fig. 10 Dynamic Effect of increase DG DC power injection

B. Three phase fault with & without DG DC power injection

From fig. 11 and 12, three phase fault is applied at t=1.7 s during 0.12 s at station 2. At this time, the transmitted DC power is almost halted and the DC voltage tends to increase since the DC side capacitance is being excessively charged. A special function (DC voltage control Override) in the Active power control (in station 1) attempts to limit the DC voltage within a fixed range. The system recovers well after the fault, within 0.5s. Figure 13 and 14 shows when 60 MW DG DC power injection and fault applied at 1.7s. From figure 13, instead of the power being halted, there was a reverse power feedback to station 1 for support and power feed to station 2 almost halted to zero.

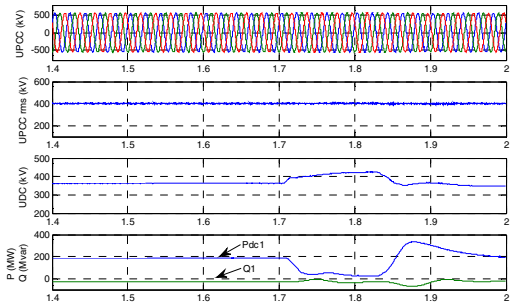

Fig. 11. Performance of the HVDC link during and after a 3-phase fault in station 2 AC grid (station 1measurement)

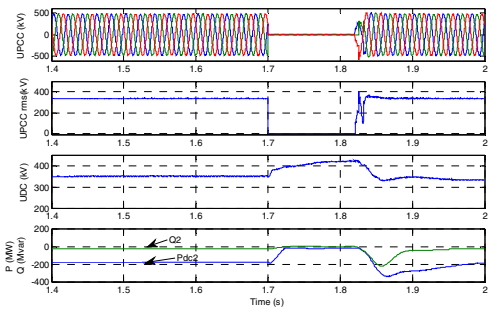

Fig. 12. Performance of HVDC link under the normal weak AC network condition during and after a 3-phase fault in station 2 grid (station 2 measurement)

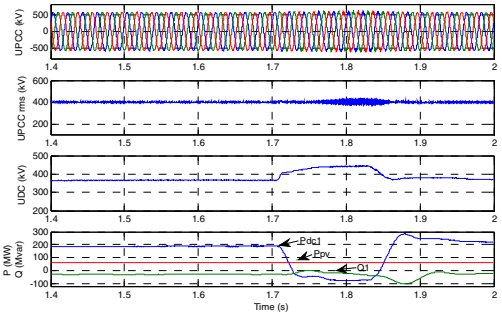

Fig. 13. Performance of HVDC link with PV penetration (60 MW) during a 3-phase fault in station 2 AC grid (station 1Measurement)

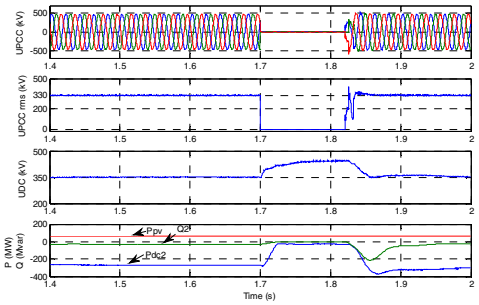

Fig. 14 Performance of HVDC link with PV penetration (60 MW) during a 3-phase fault in station 2 AC grid (station 2 Measurement)

c. Islanding condition with & without DG DC power injection

Figures 15 and 16 show the scenario at zero DC power injection and the power exported from station 1 to station 2 was about 80 MW and at 1.5s, a sudden island condition in the station 1 grid is created. The HVDC link through its control action identified the critical condition and changed the power exporting of 80 MW to importing of almost 40 MW, hence avoiding blackout.

However, when DC power injection is 60 MW, Figures 17 and 18 show how the injected DC power supported the AC system by supplying power required by station 1 and relieving station 2 from reverse power flow hence avoiding both blackout and overload on the station 1 and 2 respectively.

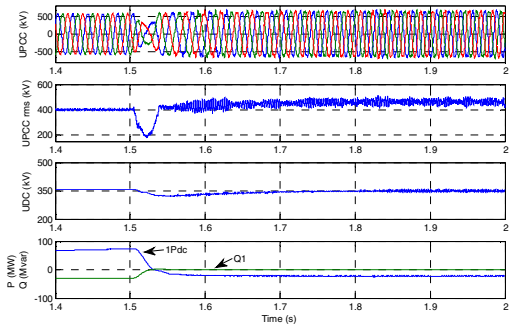

Fig.15. Performance of HVDC link under a sudden island condition in Namibia AC grid (Namibia measurement)

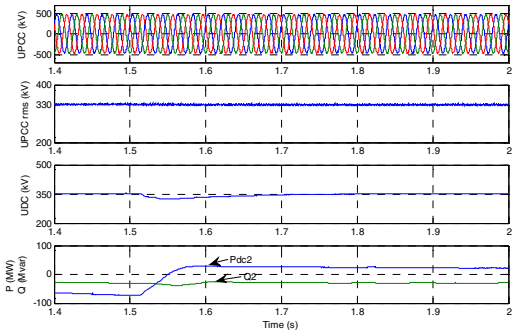

Fig.16. Performance of HVDC link under a sudden island condition in Namibia AC grid (Zambia Measurement)

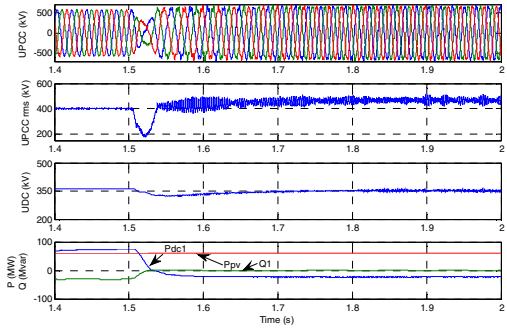

Fig.17. Performance of HVDC link with PV penetration (60 MW) under a sudden island condition in Namibia AC grid (Namibia Measurement)

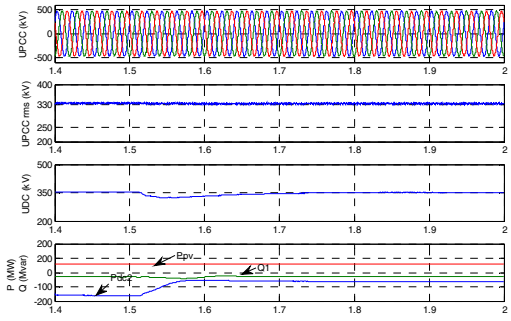

Fig. 18. Performance of HVDC link with PV penetration under a sudden island condition in Namibia AC grid (Zambia Measurement)

VI. CONCLUSION

This paper investigate the role of voltage source converter (VSC) based HVDC transmission corridor for DG power injection and for AC network stability support. A critical contingency were simulated with and without DG power injection and it was observed that the presence of DG power injection on the DC-bus supported the two weak AC sides of the system avoiding blackout and overload tripping during islanding.

REFERENCES

[1] Inigo, M. J. (2009, June). Transmission alternatives for offshore electrical power. Renewable and sustainable Energy Reviews , 13 (5), pp. 1027 - 1038.

[2] M. Durrant, H. Werner, and K. Abbott, “Model of a VSC HVDC terminal attached to a weak ac system,” in IEEE Conference on Control Applications, Istanbul, 2003.

[3] Lidong, Z., Hans-Peter, N. (2009). Multivariable Feedback Design of VSC-HVDC Connected to waek AC systems. IEEE Bucharest Power Tech Conference, june 28th – July 2nd 2009, Bucharest, Romania

[4] H. Konishi, C. Takahashi, H. Kishibe, and H. Sato, “A consideration of stable operating power limits in VSC-HVDC systems,” in Seventh International Conference on AC-DC Power Transmission, London, 2001.

[5] DU, C., Bollen, M. H., Agneholm, E., & Sannino, A. (2007). A new control strategy of a VSC-hvdc system for high quality supply of indutrial plant. IEEE Transactions on Power Delivery, 22, pp. 2386-2394.

[6] Xingjia Yao, Hongxia Sui, Zuoxia Xing, "The Study of VSC-HVDC Transmission System for Offshore Wind Power Farm," in Proc.2007 international conference on electrical machines and systems, pp.314-319

[7] Li Gengyin, Yin Ming, Zhou Ming Zhao Chengyong. "Decoupling Control for Multi-terminal VSC-HVDC Based Wind Farm Interconnection, " in Proc. 2007 Power Engineering Society General Meeting, pp.1-6

[8] Ruihua Song, Chao Zheng. "Vscs based HVDC and its Control Strategy". in Proc.2005 IEEE/PES Transmission and Distribution Conference & Exhibition, pp.1-6

[9] Jiuping P., Renaldo N., Le T., and Per H. (2008). VSC-HVDC Control and application in meshed AC network. . IEEE-PES General meeting. Pittsburgh Pennsylvania

[10] Haileselassie, T. M. (2008, june). Control of Multi-terminal VSC-HVDC Systems. *Masters thesis* .

[11] Jianhua, Z., Sheng, L., Jingfu, S., Weiwei, Z., & Chunye, L. (2008). Multi-target controller of three-level NPC Based VSC-HVDC Transmission system and its RTDS simulation. *proceedings of the ICSET*, (pp. 793-797).

[12] Temesgen H, Kjetil U and Tore U. (2009). Control of Multiterminal HVDC Transmission for Offshore Wind Energy. Nordic Wind Power Conference. Danmark.

[13] Mohamed KHATIR, Sid Ahmed ZIDI, Samir HADJERI, Mohammed Karim FELLAH. 2008. Acta Electrotechnica et Informatica Vol. 8, No. 2, 2008, 50–55

[14] A F Nnachi, Prof. J L Munda, Prof. DV Nicolae and Prof. A Mpanda Mabwe. Power sensitivity and algebraic technique for evaluation of penetration level of photovoltaic on dc link of VSC HVDC transmission. 10th International Power and Energy Conference IPEC2012, 12 -14 December 2012, Ho Chi Minh City, Vietnam

[15] Arijit, B., Arindam, m., Mark, H., & Joe, S. E. (2003). Determination of allowable penetration levels of distributed generation resources based on harmonic limit considerations. IEEE Transactions on power delivery, 18, pp. 619 - 624.

[16] Jiang-Hafner, Y., & Manchen, M. (2011). Stability Enhancement prevention by VSC Based HVDC. Electric power system of the future-Integrating supergrids and microgrids International symposium. Bologna, Italy.